CEAC-TR-00-0106

STRUCTURAL INTEGRITY OF STEEL-STRIP LAMINATE COMPOSITE PIPE FOR HIGH PRESSURE APPLICATIONS: DEFORMATION, FAILURE PREDICTION AND DESIGN VERIFICATION

S. S. Wang, X. Lu, X. H. Chen, and A. Miyase

Composites Engineering and Applications Center (CEAC),
University of Houston, Houston, TX.

NOVEMBER 2000

COMPOSITES ENGINEERING AND APPLICATIONS CENTER
FOR PETROLEUM EXPLORATION AND PRODUCTION

UNIVERSITY OF HOUSTON
HOUSTON, TX 77204-0900

CEAC-TR-00-0106

STRUCTURAL INTEGRITY OF STEEL-STRIP LAMINATE COMPOSITE PIPE FOR HIGH PRESSURE APPLICATIONS: DEFORMATION, FAILURE PREDICTION AND DESIGN VERIFICATION *

by

S. S. Wang, X. Lu, X. H. Chen, and A. Miyase

Composites Engineering and Applications Center (CEAC), and
Department of Mechanical Engineering
University of Houston
4800 Calhoun Road
Houston, TX 77204-0903

November, 2000

* Presented at the Third International Conference on Composite Materials for offshore Operation (CMOO-3), Oct.31-Nov.2, 2000, Houston, TX

ABSTRACT

In this paper, a comprehensive investigation has been made on structural integrity of the recently introduced steel-strip laminate composite pipe under combined axial and internal pressure loading. Nonlinear composite mechanics models at both ply and micromechanics levels have been developed to account for individual constituent material behavior. Advanced computational mechanics methods and algorithms have also been developed to facilitate the study of deformation, damage modes and leakage failure of the SSL composite pipe. A systematic study is conducted on the effects of different pipe diameters, number and packaging parameters of helical-wound steel strips, and the elevated temperature environment on SSL pipe degradation and leakage. Failure envelopes of SSL pipes with different sizes and steel-strip laminations are constructed for leakage-resistance design under different loading modes at room and elevated temperatures.

TABLE OF CONTENTS

1. INTRODUCTION

Fiber-reinforced polymer-matrix composites, such as glass-fiber reinforced epoxy (GRE), have been increasingly accepted for use in offshore E & P operations due to their lightweight, corrosion resistance and high specific mechanical properties. The current demand for lightweight composite pipe systems with large diameters for high pressure applications has led to the recent development of a steel-strip laminate (SSL) composite pipe, which combines the superior corrosion resistance of GRE and the high structural strength of martensitic steel and has a lower cost than that of a conventional GRE pipe, as reported in [1]. The SSL pipe has a multi-layer composite microstructure in its pipe-wall construction, including GRE inner and outer jackets, and a layer of helical-wound steel strips bonded by an epoxy adhesive sandwiched between the GRE laminates. Obviously the microstructure and constituent material systems used in the SSL composite are more complicated than those in a conventional GRE composite pipe.

Extensive experiments have been conducted to investigate and document the performance of the SSL pipe under various loading conditions at different temperatures [2]. Analytical methods have also been introduced [3] to predict the elastic response of a SSL pipe in a given loading condition. However, very limited studies have been reported on evaluation of damage modes and the leakage failure resistance envelope of a SSL composite pipe subject to general, combined axial loading and internal pressure.

Composite laminate mechanics has been an important subject for studying filament-wound thin-wall composite tubular (or cylindrical shells) under multiaxial loading during last several decades. Early studies, for example, Refs. [4,5], have reported advanced linear shell theories for thin-wall multi-layer fiber-composite pipe under general loading. In recent studies [6], nonlinear composite constitutive properties have been shown to have a significant influence on deformation and failure of composite laminate tubes subject to combined internal pressure and axial loading. Proper construction of failure envelopes for cylindrical composite laminate shells requires the inclusion of damage modes and physical mechanism-based failure criteria at the ply level to account for initiation, growth, and final failure of the composite structure. The SSL pipe is a hybrid composite system which warrants a thorough understanding of individual constituent components behavior and their contributions and interactions in the composite pipe structural integrity study.

In this study, nonlinear composite mechanics models at both ply and micromechanics levels are introduced to account for the nonlinear behavior and damage of the steel strips and the GRE composite during deformation and failure. Advanced 2D and 3D computational mechanics methods are developed to predict deformation, damage modes and growth, as well as leakage failure envelopes of the SSL pipes with different laminate constructions subject to general combined axial and pressure loading at both room and elevated temperature. Systematic and parametric numerical studies are also conducted to investigate the effects of different pipe diameters, number and packaging parameters of helical-wound steel strips, and elevated temperature environment on SSL pipe degradation and leakage failure. The results

obtained in the study provide further insight in understanding the performance and leakage resistance of the SSL pipe, and the models and methods developed are expected to aid future microstructure design and optimization, improvement of the manufacturing process, performance evaluation and prediction of the SSL pipe.

2. SSL PIPE CONSTITUENT MECHANICAL PROPERTIES AND PIPE TEST DATA

2.1 Constituent Material Properties

To study SSL pipe integrity with proper composite mechanics methodologies, mechanical properties of each constituent material at room and elevated temperatures need to be determined first. The constituent materials of a SSL pipe are: epoxy resin, strip steel, adhesive material for steel strips, and filament-wound glass/epoxy composite GRE jackets.

The epoxy resin used in the SSL composite pipe (for both glass-fiber reinforced composite laminates and adhesive material for steel strip layers) is Epon 827 with an isophorone diamine (IPD) curing agent. Typical elastic properties [7] of the epoxy resin have an elastic modulus of 360 Ksi and a Poisson's ratio of 0.37. Its ultimate tensile strength is 12.1 Ksi at failure strain 6.8% (room temperature).

The steel strip used in the SSL composite pipe study is a martensitic M190 steel with a minimum tensile strength of 190Ksi. From tensile stress strain curves of the steel [8], the constitutive equation can be approximated as bilinear. The steel strip has the following material properties: elastic modulus, 30Msi; Poisson's ratio, 0.30, and work-hardening coefficient, 5.1Msi. The mechanical properties of the steel strip are assumed to remain unchanged over the operating temperature range considered.

The adhesive material for the steel-strip layer construction is a Reemay-style 2011 nonwoven veil/epoxy. The single-ply adhesive material has been tested at room and elevated temperatures. Mechanical properties of the Reemay style 2011/epoxy adhesive are determined by experiments, and the results are given in Table 1.

The room-temperature mechanical properties (Table 2) of a similar filament-wound glass/epoxy composite (GRE) obtained in a previous research [6] are used for the subsequent SSL pipe modeling and analysis.

To determine the composite material behavior at high temperatures, hoop-wound glass/epoxy tubular specimens, using the same material system as those in a SSL composite pipe have been tested under selected loading modes. Stress-strain curves under monotonic axial tension and pure in-plane shear at different temperatures are obtained and shown in Figs. 1 and 2, respectively. The composite elastic modulus decreases with an increase in temperature. The degree of shear non-linearity increases with temperature. A nonlinear constitutive material equation, based on the complementary strain energy density approach [9], is used to model the nonlinear shear behavior of the GRE composite, i.e.,

$$\gamma_{12} = \frac{\tau_{12}}{G_{12}} + S_{6666}(\tau_{12})^3 \qquad (1)$$

where γ_{12} is the engineering shear strain, and G_{12} and S_{6666} are the linear shear modulus and the nonlinear shear coefficient, respectively. The mechanical property data determined experimentally for the hoop-wound glass/epoxy composite are summarized in Table 3.

Straight-sided (4-ply) steel-strip/epoxy specimens have been tested to determine their mechanical behavior (Fig. 3). The elastic properties (Table 4) determined from the experiments are in good agreement with the analytical predictions, using the micromechanics model for a ribbon-reinforced composite [10]. Failure strength of the steel-strip/epoxy lamina specimens, however, is found to be significantly lower than its strength value (110 Ksi) back calculated from the carefully conducted SSL pipe tests. Therefore, the failure strength of the steel strip/epoxy lamina determined analytically from the SSL composite pipe tests is used for the subsequent modeling and progressive failure analysis.

2.2 SSL Composite Pipe Test Data

Carefully conducted tests on SSL composite pipes with different diameters and steel-strip layer constructions have been performed at Ameron under hoop-to-axial loading ratios of 2:1 at 70 °F and 200°F, and 0:1 at room temperature. During the tests, hoop and axial strains and internal pressure have been recorded. Details of the SSL pipe configurations, steel-strip constructions, test conditions, and failure pressure are summarized in Table 5.

3. ANALYTICAL MODELING AND METHODS OF ANALYSIS

3.1 Thin-Shell Composite Laminate (CLT) Modeling and Analysis

Consider a thin cylindrical composite laminate shell (Fig. 4). The displacements of its mid-plane are denoted by u_0, v_0, and w_0. Based on the well-known Kirchhoff hypothesis, the in-plane displacements, u and v, in axial and circumferential directions, respectively, at any distance z from the mid-plane are given by

$$\begin{aligned} u &= u_0 - z\,\partial w/\partial x \\ v &= v_0 - z\,\partial w/R\partial\theta \end{aligned} \tag{2}$$

where w is the displacement in the z direction with $w = w_0$ from the thin-shell plane-stress approximation. Individual ply strains are then obtained in terms of the middle-plane strain ε_0 and curvatures κ_i as

$$\varepsilon_i = \varepsilon_0 - z\kappa_i \tag{3}$$

where ε_i are strains given as

$$\varepsilon_x = u_{,x}, \quad \varepsilon_\theta = (v_{,\theta} + w)/R, \quad \varepsilon_{x\theta} = u_{,\theta}/R + v_{,x}, \tag{4a-c}$$

The κ_i are the composite laminate curvatures expressed as

$$\kappa_x = -w_{,xx}, \quad \kappa_\theta = -(w_{,\theta\theta} + w)/R^2, \quad \kappa_{x\theta} = -(2w_{,x\theta} + u_{,\theta}/R - v_{,x})/R. \tag{5}$$

Each individual ply in the cylindrical composite laminate is assumed to be transversely isotropic in its principal material coordinates. Using appropriate transformations, one may determine the stress-strain relationship of the k-th ply in the fiber-composite laminate in global (x,θ,z) coordinates as

$$\sigma_i^{(k)} = \overline{Q}_{ij}^{(k)} \varepsilon_j. \quad (i,j = 1, 2, 6) \tag{6}$$

where $\overline{Q}_{ij}^{(k)}$ is the stiffness of the ply in global coordinates. Resultant forces, **N**, and moments, **M**, per unit length acting on the composite laminate are obtained by integration of ply stresses through the laminate thickness as

$$N_i = \int_{-h/2}^{h/2} \sigma_i dz, \qquad M_i = \int_{-h/2}^{h/2} \sigma_i z dz, \qquad (i = 1,2,6) \tag{7}$$

Equations (3) and (6) in conjunction with Eqs. (7) yield the constitutive equations for the composite laminate in the form,

$$\begin{Bmatrix} \mathbf{N} \\ \mathbf{M} \end{Bmatrix} = \begin{bmatrix} \mathbf{A} & \mathbf{B} \\ \mathbf{B} & \mathbf{D} \end{bmatrix} \begin{Bmatrix} \varepsilon^{o} \\ \kappa \end{Bmatrix} \tag{8}$$

where **A** is the extensional stiffness matrix, **D** the bending stiffness matrix, and **B** the coupling stiffness matrix. For a thin-wall composite laminate pipe of a sufficiently long length, the stress field in the composite laminate pipe can be obtained as [6]

$$\sigma_i = \overline{Q}_{ij}\left[\frac{b_{jk}^{\ 0}}{t} N_k\right] + \frac{z}{Rt}\left(\overline{Q}_{i6} b_{6j}^{\ 0} - \overline{Q}_{i2} b_{2j}^{\ 0}\right) N_j . \tag{9}$$

Summation is applied to the repeated indices in Eq. (9), and t is the thickness of the composite laminate tube. The $b_{ij}^{\ 0}$ is the inverse of the b_{ij} matrix, which can be shown as

$$b_{ij} t = A_{ij} + \frac{1}{R}\begin{bmatrix} 0 & -B_{12} & B_{16} \\ 0 & -B_{22} & B_{26} \\ 0 & -B_{26} & B_{66} \end{bmatrix}. \tag{10}$$

The steel-strip/epoxy lamina in the SSL composite pipe is assumed as a structural load-bearing layer of approximately isotropic stiffness with a linear plastic hardening. In the computational algorithm development, an iteration method with a total secant stiffness approach has been used for modeling the nonlinear GRE composite laminate and the elastoplastic steel-strip/epoxy lamina layer.

3.2 3D Micromechanical Modeling & Analysis

An advanced 3-D computational mechanics model has also been developed in this study to account for micromechanical details of deformation and failure of the GRE plies and the steel-strip/epoxy layer in the SSL pipe body subject to multiaxial loading. The formulation includes the helical steel strips with plastic yielding, the epoxy gap-filler and adhesive with nonlinear elasticity, and the GRE inner plies and outer jacket with transversely isotropy and shear nonlinearity. The formulations are then incorporated into the displacement-based, finite-element procedure in an ABAQUS program. The three-dimensional displacement solution is constructed as a sum of a homogeneous solution and a particular solution in the helical coordinates along the steel strip. Eight-node iso-parametric elements with nine Gauss integration points are employed to calculate all six components of the total strain (or stress). Periodic boundary conditions are applied to the representative cell in the micromechanics formulation with constraint equations.

The SSL pipe has a sandwich-type structure, consisting of a GRE (fiberglass reinforced epoxy) inner liner, steel strip layers and a GRE outer jacket. Steel strips are wound at a very low certain helical angle with the selected epoxy as a gap filler and an adhesive layer. The 3-D geometry and the cross section at $\theta=0^{o}$ of the SSL pipe body with an inner diameter of

8.22 inch and a pitch of 4.176 inch are shown in Fig.5 with its geometric parameters listed in Tables 6 and 7.

Elastoplastic yielding with a linear isotropic hardening is used in the formulation for the steel-strip/epoxy lamina layer, i.e.,

$$\sigma = \frac{1}{\frac{1+\nu}{E} + \frac{3}{2}\frac{(\sigma_s - \sigma_y)\mathrm{H}(\sigma_s - \sigma_y)}{G_H \sigma_s}}\left(\varepsilon - \frac{1}{3}\mathbf{I}\mathbf{I}:\varepsilon\right) + \frac{1}{3}\frac{E}{1-2\nu}\mathbf{I}\mathbf{I}:\varepsilon \tag{11}$$

where ε is the strain tensor; σ is the stress tensor; $\mathbf{e}$ is the strain deviator; $\mathbf{I}$ is the second-order unit tensor; σ_s is von Mises equivalent stress; $\bar{e}$ is an equivalent strain; E is the Young's modulus; ν is the Poisson's ratio; σ_y is the yield strength; G_H is the hardening modulus, and H is the Heaviside function defined as follows:

$$\mathrm{H}(\sigma_s - \sigma_y) = \begin{cases} 0 & \text{as } \sigma_s < \sigma_y \\ 1 & \text{as } \sigma_s \geq \sigma_y \end{cases}$$

Nonlinear elasticity formulation, based on the Ramberg-Osgood model, is used for modeling the epoxy gap filler and the adhesive between the steel strips

$$\varepsilon = \frac{1+\nu}{E}\sigma - \frac{\nu}{E}\mathbf{I}\otimes\mathbf{I}:\sigma + \frac{3}{2E}S_n\sigma_s^{n-1}\left(\sigma - \frac{1}{3}\mathbf{I}\otimes\mathbf{I}:\sigma\right) \tag{12}$$

where n is the hardening exponent, $S_n = \alpha/\sigma_0^{n-1}$, α and σ_0 are material parameters in the Ramberg-Osgood model. Material properties in Eq. (12) obtained from the experiments discussed in the previous section are given in Table 8.

The boundary value problem for a SSL composite pipe body with a helical, periodic microstructure is solved with the following transformations between the helical coordinates $\{r,\xi,\eta\}$ and the cylindrical coordinates $\{r,\theta,z\}$ (Fig.5):

$$r = r, \quad \xi = r\theta\cos\alpha - z\sin\alpha, \quad \eta = r\theta\sin\alpha + z\cos\alpha \tag{13}$$

where α is the helical angle.

For the SSL composite pipe problem, the three-dimensional displacement field is expressed by

$$\begin{aligned} \hat{u}_r(r,\xi,\eta) &= \hat{u}_r^0(r,\xi) \\ \hat{u}_\xi(r,\xi,\eta) &= \hat{u}_\xi^0(r,\xi) + (\Theta r\cos\alpha - \bar{\varepsilon}_z\sin\alpha)(\eta\cos\alpha - \xi\sin\alpha) \\ \hat{u}_\eta(r,\xi,\eta) &= \hat{u}_\eta^0(r,\xi) + (\Theta r\sin\alpha + \bar{\varepsilon}_z\cos\alpha)(\eta\cos\alpha - \xi\sin\alpha) \end{aligned} \tag{14}$$

where the homogeneous solution with the superscript '0' depends only on variables r and ξ. The particular solution can be expressed by an average axial strain $\bar{\varepsilon}_z$ and twisted angle per unit length, Θ, in the nominal region.

Helical periodic conditions are applied at the two sides $\xi = \xi_1$ and $\xi = \xi_2$ with $\xi_2 = \xi_1 + b$ as

$$\hat{u}_r^0(r,\xi_1) = \hat{u}_r^0(r,\xi_2), \quad \hat{u}_\xi^0(r,\xi_1) = \hat{u}_\xi^0(r,\xi_2), \quad \hat{u}_\eta^0(r,\xi_1) = \hat{u}_\eta^0(r,\xi_2) \tag{15}$$

The applied internal and external pressures at the inner and outer walls at $r = r_1$ and $r = r_2$ are

$$\hat{\sigma}_r^0(r_1,\xi) = -p_1, \quad \hat{\sigma}_r^0(r_2,\xi) = -p_2 \tag{16}$$

Either average deformation ($\bar{\varepsilon}_z$, Θ) or total load (P_z, T_z) may be specified as the end conditions at a dummy node with two active degrees of freedom, i.e.,

$$\bar{\varepsilon}_z = \varepsilon_{z0} \quad \text{or} \quad P_z = P_0, \qquad \Theta = \Theta_0 \quad \text{or} \quad T_z = T_0 \tag{17}$$

3.3 Failure Criteria for Progressive Damage and Leakage Failure Analysis

In this study, the following physical mechanism-based failure criteria have been used in deformation analysis and failure prediction for the GRE plies.

1) Fiber-dominated ply fracture: The well-known maximum stress criterion is used to predict the fiber-dominant ply failure.

2) Matrix-dominated ply cracking: The recently developed 3-region failure criteria [6] are employed for predicting matrix cracking in the GRE composite ply. In formulation of the criteria, interactions between transverse and shear stresses are included. Failure modes between the combined tension-shear case and the compression-shear case are distinguished.

3) SSL ply yielding and fracture: The well-known von Mises criterion is used for modeling the SSL ply plastic yielding. Along the transverse direction of the steel-strip/epoxy lamina, the maximum stress criterion is used to predict SSL debonding.

Mechanical property degradation of individual plies in the SSL composite laminate pipe may occur as the internal ply damage accumulates during the load increase. In this study, an instantaneous ply unloading model proposed by Chiu [11] has been applied in the progressive failure analysis of the SSL composite pipe. The ply degradation model assumes that a composite ply loses its entire load-carrying capacity immediately after the ply failure. It is recognized that the approach provides a conservative model for evaluating the damage evolution in the SSL composite pipe.

The mechanical behavior of the steel strip/epoxy ply may also be degraded when plastic yielding occurs in steel strips. This form of degradation is modeled with an elastoplastic linear hardening scheme, based on the experimental results of the steel-strip composite tests.

4. RESULTS AND DISCUSSION

4.1 Deformations and Progressive Damage Modes

The analytical methods and associated computational procedure developed have been used to evaluate the safe design of the SSL composite pipe body at both room and elevated temperatures. Both experimental and analytical results are shown here for deformations and leakage failure of a SSL composite pipe made of a 4-steel strip/epoxy lamina with a 10-inch nominal diameter subjected to combined internal pressure and axial tension. The SSL composite pipe has an inside GRE jacket with a thickness of 0.153 inch, an outside jacket of 0.081 inch, and a 4-strip steel-strip/epoxy lamina of 0.088 inch thickness. The adjacent steel strips have a gap of 0.002 inch filled with glass flakes and an epoxy adhesive. Surfaces of the steel strips are sandblasted before wounded into the composite pipe.

In Figs. 6, hoop and axial deformations are obtained from the analysis and shown for the 10 inch-diameter SSL pipe subjected to combined (2:1) hoop and axial loading at room temperature and 200°F. Also, experimental data from strain gage measurements are shown in the figures for comparison. Good agreement between the analytical predictions and the test results of the SSL deformation is observed.

The analytical results also reveal the progressive damage growth and associated failure mode development in the SSL pipe. The results indicate that the first damage initiates in a tensile ply matrix-cracking mode in the GRE jackets, followed by plastic yielding in the steel-strip/epoxy lamina. The final pipe leakage occurs after transverse fracture of the steel strip/epoxy lamina. The instantaneous unloading model used in the current ply property-degradation model is noted to cause a jump in the prediction of hoop deformation at the pressure around 3.6 ksi.

4.2 SSL Composite Pipe Failure Modes and Leakage-Failure Envelopes

The failure modes and leakage-failure envelope of the 10-inch-diameter SSL composite pipe have been predicted and shown in Figs. 7. In the figures, distinct regions of ply matrix cracking in the GRE jackets and steel-strip/epoxy layer plastic yielding during the SSL pipe failure are identified. It is clearly seen that along the pipe failure envelope, different failure modes occur, leading to the final leakage of the SSL pipe body. For example, when a SSL pipe is subjected to a combined high internal pressure and axial tensile loading, leakage in the pipe body is mainly caused by the steel strip/epoxy layer yielding, followed by ply-matrix cracking in the GRE laminate, resulting in the final fiber breakage of the composite ply. The ply matrix cracking and SSL layer fracture are responsible for the leakage when an axial tension becomes dominant. On the other hand, when the SSL composite pipe is subject to a combined high internal pressure and high axial tension, GRE ply-matrix cracking, and subsequent steel-strip/epoxy layer plastic yielding and fracture will result in the final pipe leakage. We note that the predicted leakage failure loading has been confirmed by the actual test data as shown in the Figures.

4.3 Effect of SSL Pipe Diameter on Leakage Resistance

The important issue of the effect of SSL pipe diameter on leakage failure has been investigated thoroughly. Four distinct steel-strip configurations with five different pipe diameters are considered. The nominal pipe diameters chosen for the study are: 8", 10", 14", 20" and 32", respectively. The numbers of steel strips in the SSL layer of the pipe are: 3, 4, 6, and 8. For each case investigated, an inside GRE jacket thickness of 0.12 inch and an outside jacket of 0.060 inch thick are used. The space between the adjacent steel-strips is 0.006 inch, filled with Reemay veil and epoxy adhesive resin. The strip-steel/epoxy lamina thickness is 0.020 inch with the surface of the individual steel strip being sandblasted.

In Fig. 8, the predicted leakage failure envelopes are shown for 3-strip SSL composite pipes with different diameters. As anticipated, a small-diameter SSL pipe has a high-pressure resistance but low axial-load bearing capacity. When expressing the failure envelopes in Fig. 8 based on average pipe wall stress (Fig. 9), one recognizes that, for different size SSL pipes with a given number of steel strips, the leakage failure envelopes are independent of pipe diameters. Based on this finding, it becomes evident that only one unique failure envelope exists for all SSL pipes of different diameters (with a given number of steel strips).

4.4 Effect of Number of Steel Strip Layers

In Fig. 10a, the leakage failure envelopes are shown for the SSL composite pipes with different steel-strip constructions (3, 4, 6, and 8-strips). The axial load bearing capacity of the SSL pipe with a high number of steel strips is found to increase less significantly as the pressure resistance of the pipe with a low number of steel strips.

4.5 Effect of Temperature

Similar to the room-temperature cases studied, the SSL pipes containing four steel-strip/epoxy configurations with five different diameters are investigated here. Note that the steel strip/epoxy systems considered here are different from those used in the SSL pipes at room temperature. Here the inter-strip space between the steel layers is 0.002 inch, filled with glass flakes and an epoxy adhesive resin. The surface of the steel strip is gel-coated. In Fig. 10b, leakage failure envelopes of SSL composite pipes with 3, 4, 6, and 8-strip steel constructions at 200°F are shown. Comparing with Fig. 10a, one finds that the SSL pipes at elevated temperature have higher failure strengths mainly due to the smaller gap between the steel-strip layers and slightly higher SSL debonding strength at 200°F.

4.6 Microscopic Stress Concentrations and Localized Yielding in Steel Strip/Epoxy Layer

In this section, only limited results of the local stress concentration and microscopic yielding in the steel-strip/epoxy layer of an 8"-diameter SSL Pipe with a 3-steel-strip construction are reported due to space limitation. The 3D micromechanical model and the

method of analysis developed should be useful for future use in guiding the microstructure design optimization, manufacturing, and performance evaluation of the SSL pipe.

The results presented in the previous section clearly indicate the importance of the steel strip/epoxy layers in the load-carrying capability of the SSL composite pipe. It becomes critical to devise an effective method to analyze and understand the local stress concentrations and plastic yielding in the steel-strip layers in the pipe. An advanced micromechanics model and analysis method have been developed in this research and reported in detail elsewhere [12]. The micromechanics model and the associated method of analysis are formulated by the use of a homogenization theory to account for the periodical helical microstructure of the steel strips and the surrounding epoxy adhesives. Nonlinear plastic yielding and flow as well as the nonlinear elastic constitutive behavior of the steel strips and the adhesive epoxy are included in the formulation. The aforementioned homogenization theory is used in conjunction with a quasi 3D (finite-element) computational mechanics algorithm for analyzing the deformation, yielding, damage and local failure of the steel-strip/epoxy layer in the SSL pipe under axial tension and internal pressure.

A finite element discretization is made for the SSL pipe body containing three steel strips with a pitch length of 4.176 inches (60,610 elements and 184,038 nodes). A special quasi 3-D helical element is developed in the study to account for the geometry & configuration of the steel strips in the pipe. Von Mises stress and other selected stress components are obtained in a helical coordinate system of the SSL pipe under axial loading and internal pressure are shown in Figs.11 and 12. The critical shear stress transfer in the epoxy adhesive between the steel strips along Sections 4 and 5 is clearly shown in Figs.13 (a) and (b). Very high shear stress concentrations are observed in the epoxy adhesive near the edges of the steel strip.

The von Mises stresses for steel yielding along different sections specified in Fig.7 are shown in Figs.14 (a) and (b). The dramatic differences in material properties of the steel strip, the epoxy adhesive, and the GRE inner and outer jackets lead to high stress concentrations and significantly different stress states. The influence of the edge geometry of the steel strip is obvious. As expected, severe stress concentrations occur in the epoxy adhesive around the steel strip with sharp stress transfer jumping across the steel-epoxy interface. Steel strip plastic yielding occurs before the SSL pipe leaks in the case of internal pressure loading, whereas no yielding is found prior to the SSL pipe failure in a pure axial tension case.

5. CONCLUSIONS

A comprehensive study has been conducted on deformation, damage and failure behavior of the recently introduced SSL composite pipe. Advanced nonlinear composite mechanics models and computational mechanics methods have been developed in the study to facilitate the investigation. Based on the results obtained, the following conclusions may be drawn.

(1). Deformation, damage modes and leakage of a SSL pipe can be accurately modeled and predicted, using the advanced composite mechanics models and methods developed in the study. The predictions have also been confirmed by carefully conducted experiments.

(2). A leakage failure envelope can be analytically constructed for safe design of a SSL composite pipe body against any combinations of applied axial loading and internal pressure.

(3). Three distinct failure processes in a SSL pipe can be identified for each combined external loading state. These processes include: (1). GRE ply matrix cracking and steel-strip layer fracture; (2). GRE ply matrix cracking, steel-strip layer yielding, and steel-strip layer transverse fracture, and (3). GRE ply matrix cracking, steel-strip layer yielding, and GRE ply fracture with a fiber-dominant mode.

(4). The contributions of helical-wound steel strip layers are critical in *all* cases of externally applied axial and pressure loading. However, the nature of the contribution in each case is dependent upon the individual combination of axial stress and internal pressure. For example, in the case involving high axial loading, the leakage failure of a SSL pipe is governed by the transverse fracture strength of the steel strip/epoxy layer.

(5). The contribution of the GRE laminate to leakage failure of a SSL pipe is also critical. Transverse ply matrix cracking occurs first in all cases of combined axial loading and internal pressure. However, leakage of a SSL pipe under external loading involving high internal pressure is governed by the fiber fracture strength of GRE composite plies.

(6). Based on the pipe-wall stress representation, a unique leakage failure envelope can be constructed for SSL pipes of all sizes, independent of the pipe diameter, provided that the number of wound steel strips remains the same. Thus, the common concern of size effect on pipe pressure rating should not be an issue in the safe design of SSL pipe.

(7). The number of steel-strip layers wound into the SSL composite during pipe body construction governs the leakage-failure resistance capacity of the pipe. However, the improvement of leakage resistance by introducing additional steel strips in a SSL pipe is more effective for the cases involving high axial loading than those with high internal pressure, whereas the opposite is true for the cases involving both high pressure and high axial tension.

(8). Based on the results from the SSL systems discussed in Figs. 10a and 10b, the SSL composite pipe with a given number of steel strips wound in it has a larger leakage failure envelope, i.e., better leakage resistance, at a higher temperature than that at room temperature

– a unique feature which does not generally appear in most fiber-reinforced polymer composite pipes.

(9). The nonlinear 3-D micromechanics model and advanced computational methods enable us to model precisely the local stress concentrations, plastic yielding and deformation, and damage growth in the helical steel strips, adhesive epoxy bond layers, and individual GRE plies in a SSL pipe under combined axial and pressure loading. The analytical models and methods developed here and the results obtained are important for future microstructural design and optimization, manufacturing process improvement, and performance and reliability evaluation of the SSL composite pipe.

6. ACKNOWLEDGEMENT

The research reported in this paper was supported by a grant from Ameron International to the Composites Engineering and Applications Center (CEAC) at the University of Houston. The authors wish to express their gratitude to Mr. Gordon G. Robertson and Mr. Rocky Friedrich of Ameron for their encouragement, advice and fruitful discussion during the course of the study. Dr. Qizhong Sheng of Ameron is also gratefully acknowledged for providing some of the important material test data for the project.

7. REFERENCES

[1] R. Friedrich, "Steel Strip Laminate – A New High Performance, Hybrid Composite Pipe", *Composite Materials for Offshore Operations*-2, edited by S. S. Wang, J. G. Williams and K. H. Lo, Eds., ABS Publishing, New York, 1999, p183-196.

[2] R. Friedrich, S, Hall, Q. Sheng, K. Smyth, and D. Wang, "Preliminary Status Report, Steel Strip Laminate Pipe (SSL) Development Project", Ameron International, 1998.

[3] *SSL Pipe Design Book*, Ameron International, 1999.

[4] G. C. Eckold, D. Leadbetter, P. D. Soden and P. R. Griggs, "Lamination Theory in the Prediction of Failure Envelopes for Filament Wound Materials Subjected to Bi-axial Loading," *Composites*, Vol. 9, pp. 243-246 (1978).

[5] J. M. Whitney and J. C. Halpin, "Analysis of Laminated Anisotropic Tubes under Combined Loading," *Journal of Composite Materials*, Vol. 2, pp. 360-367 (1968).

[6] S. S. Wang and S. Srinivasan, "Long-term Leakage Failure of Filament-wound Fiberglass Composite Laminate Tubing under Combined Internal Pressure and Axial Loading", *Technical Report CEAC-TR-96-0101*, University of Houston, December 1996.

[7] *Epon Resin Structural Reference Manual - Materials Selection by Performance Properties*, Shell Chemical Company, 1981, pp. 79.

[8] S. S. Wang and A. Miyase, "Deformation And Leakage: Failure Of Steel-Strip Laminate (SSL) Composite Pipe, Part 1: Constituent Material Properties", *CEAC Technical Report*, University of Houston, 2000.

[9] H.T. Hahn and S.W. Tsai, "nonlinear elastic behavior of unidirectional composite laminae", *Journal of Composite Materials*, Vol. 7, 1973, pp. 102-118.

[10] J.C. Halpin and R.L. Thomas, "Ribbon Reinforcement of Composites", *Journal of Composite Materials*, Vol.2, 1968, pp. 488-497.

[11] K. D. Chiu, "Ultimate Strengths of Laminated Composites," *Journal of Composite Materials*, Vol. 3, pp. 578-582 (1969).

[12] S. S. Wang and X. H. Chen, "Deformation And Leakage: Failure Of Steel-Strip Laminate (SSL) Composite Pipe, Part 3: 3-D Nonlinear Micromechanics Modeling of Local Stress Concentrations, Plastic Yielding, and Failure", *CEAC Technical Report*, University of Houston, 2000.

8. TABLES

Table 1. Mechanical properties of Reemay type 2011/epoxy at different temperatures

	70°F	150°F	200°F
E (Msi)	0.380	0.290	0.274
UTS (Ksi)	6.0	5.4	3.6

Table 2. Room-temperature mechanical properties of filament-wound glass/epoxy composite used for SSL pipe modeling and analysis

E_{11} (Msi)	E_{22} (Msi)	ν_{12}	G_{12} (Msi)	S_{6666} $(psi)^{-3}$	X_1^+ (Ksi)	X_1^- (Ksi)	X_2^+ (Ksi)	X_2^- (Ksi)	X_6^- (Ksi)
7.0	1.9	0.313	0.83	1.65E-14	110	100	6.86	-22.00	10.60

Table 3. Properties of filament-wound glass/epoxy composite at different temperatures

Temp.	E_{11} (Msi)	E_{22} (Msi)	ν_{21}	G_{12} (Msi)	S_{6666} $(psi)^{-3}$	X_1^+ (Ksi)	X_1^- (Ksi)	X_2^+ (Ksi)	X_2^- (Ksi)	X_6 (Ksi)
70°F	(7.0)	1.71	0.103	0.95	1.5E-14	(130)	(110)	5.21	-16.5	10.5
150°F	(7.0)	1.47	0.085	0.84	2.4E-14	(130)	n/a	3.93[*1]	-15.1	8.7
200°F	(7.0)	1.39	0.074	0.79	2.9E-14	(130)	n/a	4.14	-12.1	7.4

(assumed), n/a: not available, [*1]: grip end failure.

Table 4. Comparison of experimentally determined steel-strip/epoxy lamina elastic properties with micromechanics predictions (room temperature)

	Experiment	Prediction
E_{22} (Msi)	22.5	23.8
ν_{21}	0.275	0.302

Table 5. Selected SSL composite pipe test results (conducted at Ameron)

I.D. (in)	O.D. (in)	t GRE1 (in)	t GRE2 (in)	No. of SS Layer	SS Staggering Pattern	Filler for Adhesive	Test Tem. (°F)	Hoop to Axial Load Ratio	Pressure at Failure (Psi)	No. of Tests
9.815	10.459	0.153	0.081	4	[*1]	Glass Flake	70	2:1	5415	8
9.815	10.459	0.153	0.081	4	[*1]	Glass Flake	200	2:1	6437	2
9.815	10.285	0.108	0.061	3	[*1]	Glass Flake	70	1:0	5750	1
6.225	6.729	0.116	0.070	3	[*2]	Glass Flake	70	2:1	8400	1
6.225	6.729	0.116	0.070	3	[*2]	Glass Flake	70	0:1	239Kips	1
13.56	14.168	0.120	0.080	4	[*3]	Reemay	70	2:1	3669	1
8.225	8.833	0.120	0.080	4	[*3]	Reemay	70	2:1	5786	1

[*1]: RO half/quarter, [*2]: 1/3 indexing, [*3]:standard 4/9

Table 6. Layout of a SSL pipe with an inner diameter of 8.22" and a pitch of 4.176"

	Thickness (inch)	Winding angle
GRE inner liner	0.120	$(\pm 54^\circ)_4$
Steel-strip layer	$0.022n - 0.002$	$(9^\circ)_n$
GRE outer jacket	0.060	$(\pm 54^\circ)_2$

Table 7. Geometric parameters for steel-strip layer

S. S. width	Intra-layer S. S. gap	Inter-layer S. S. gap	No. of S. S.	S. S. Staggering
4.0 inch	0.125 inch	0.002 inch	3	1/3

Table 8. Material parameters for epoxy gap filler and adhesive

E	υ	σ_0	n	α
0.36 Msi	0.37	3.08 ksi	3	0.1

9. FIGURES

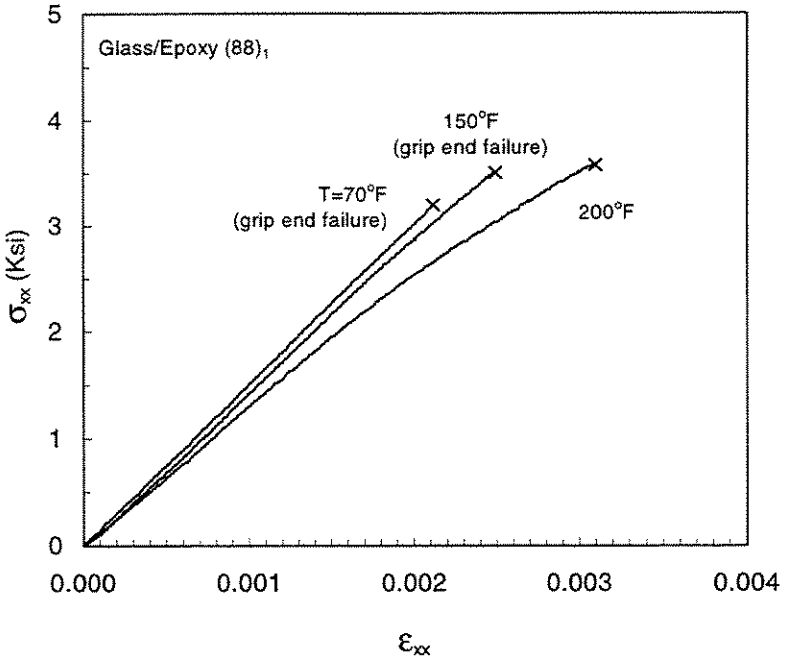

Fig. 1. Axial tensile stress-strain behavior of hoop-wound glass/epoxy composite at different temperatures.

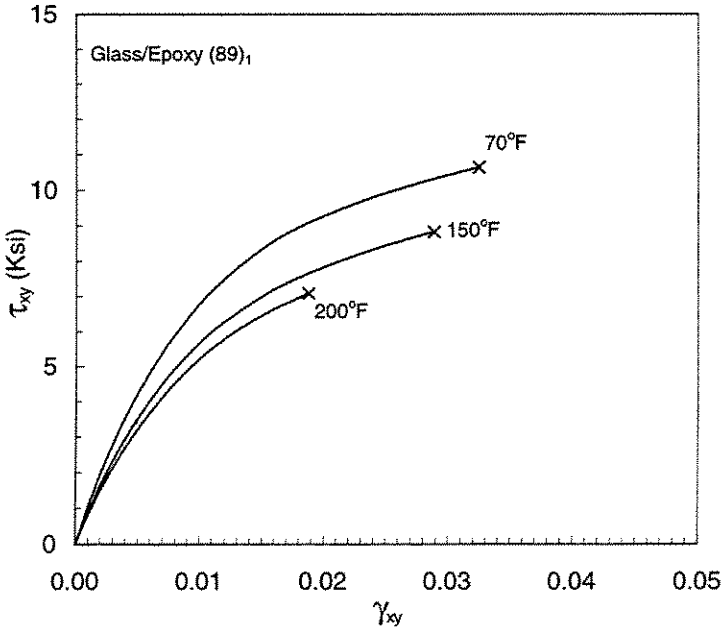

Fig. 2. Inplane shear stress-strain behavior of hoop-wound glass/epoxy composite at various temperatures.

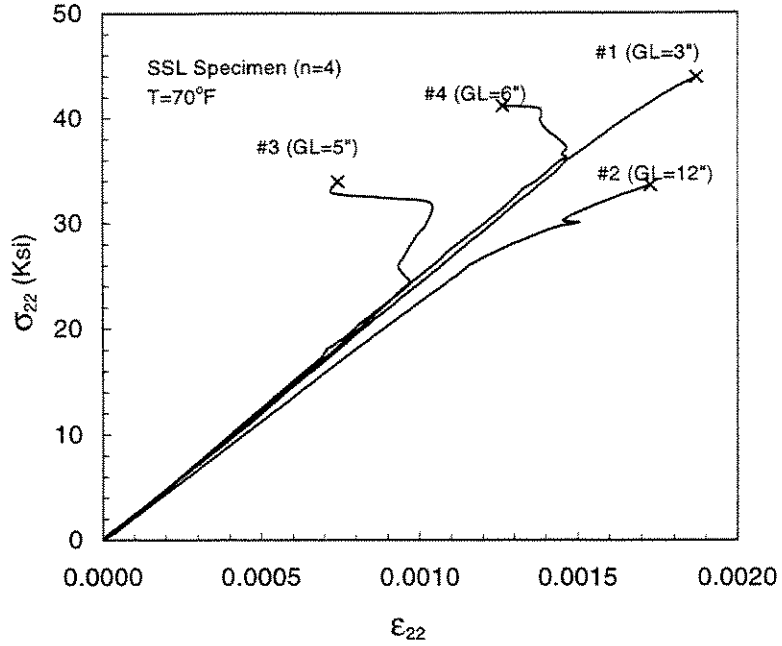

Fig. 3. Tensile stress-strain behavior of (4-ply) steel-strip/epoxy lamina specimen under uniaxial tension at 70°F.

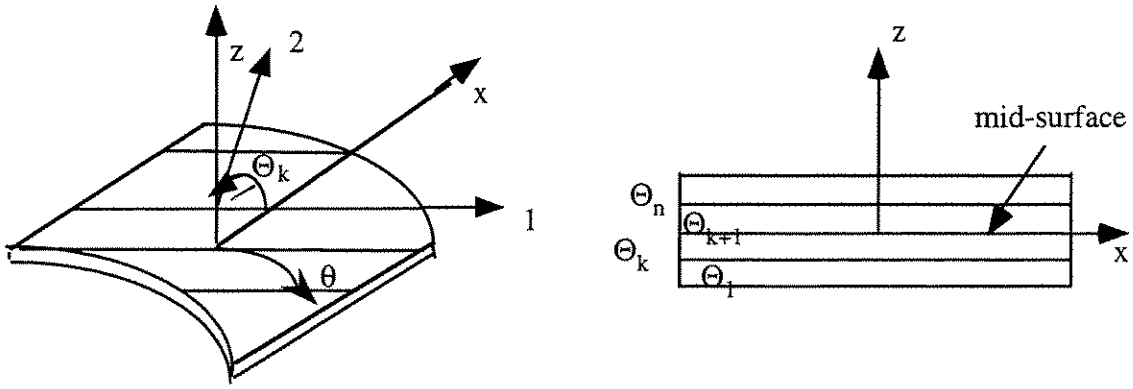

Fig. 4. Coordinates and ply fiber orientations in a composite laminate shell.

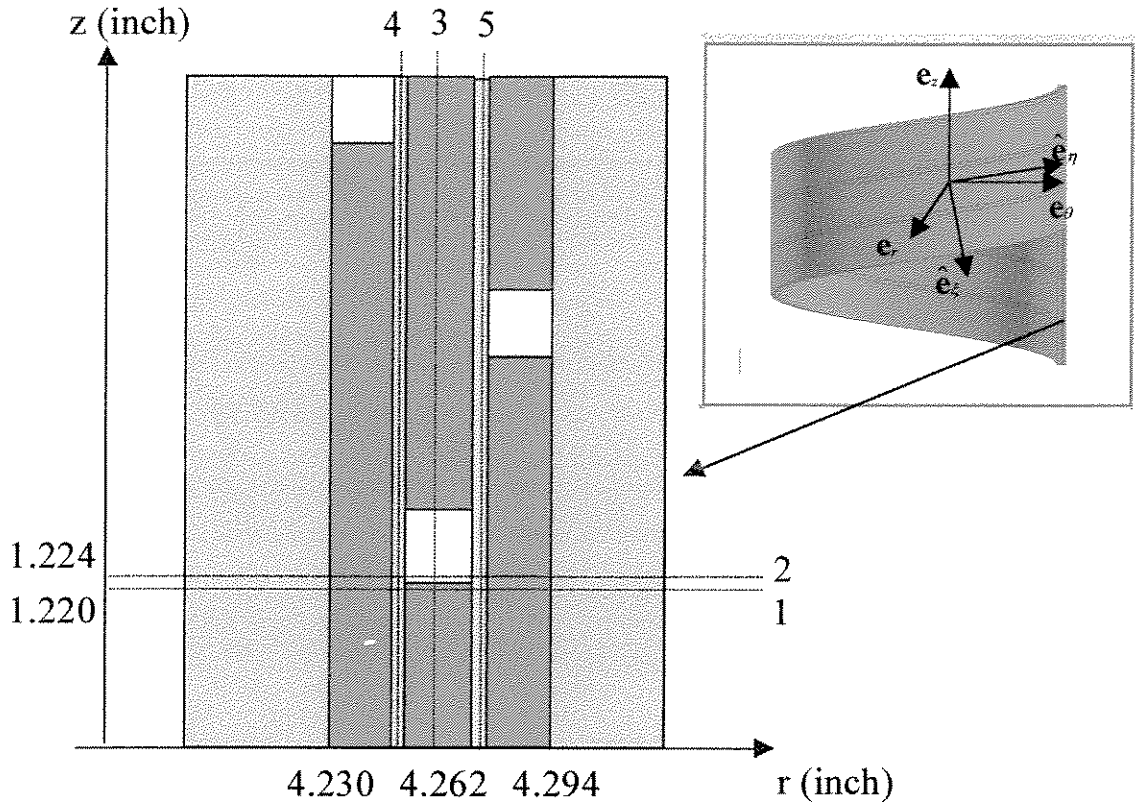

Fig.5. 3-D geometry and cross section at $\theta=0^{o}$ of a SSL pipe body.

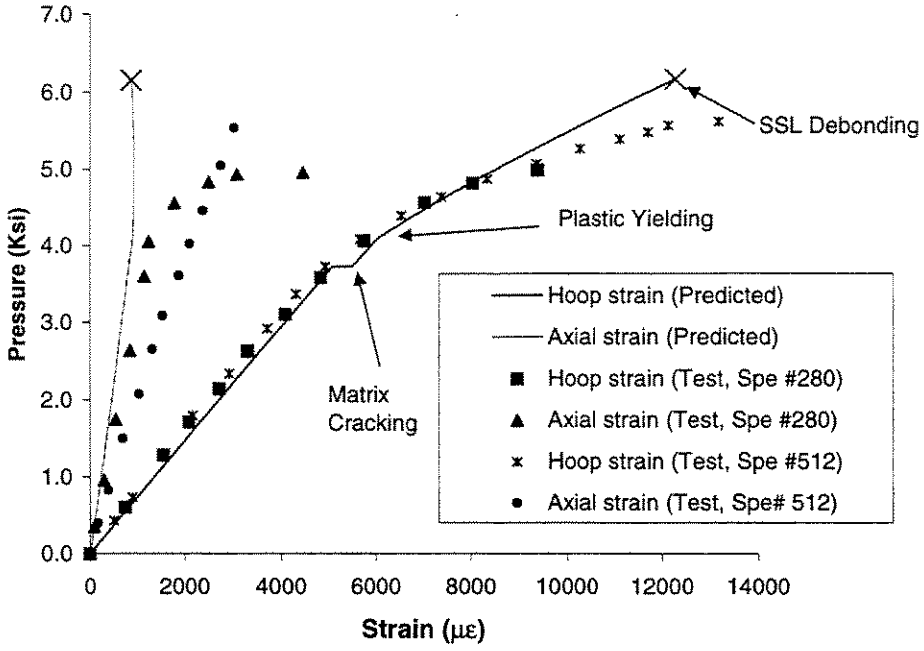

Fig. 6a. Pressure-deformation relationship in 10" 4-strip SSL pipe subjected to combined 2:1 hoop and axial loading (70°F).

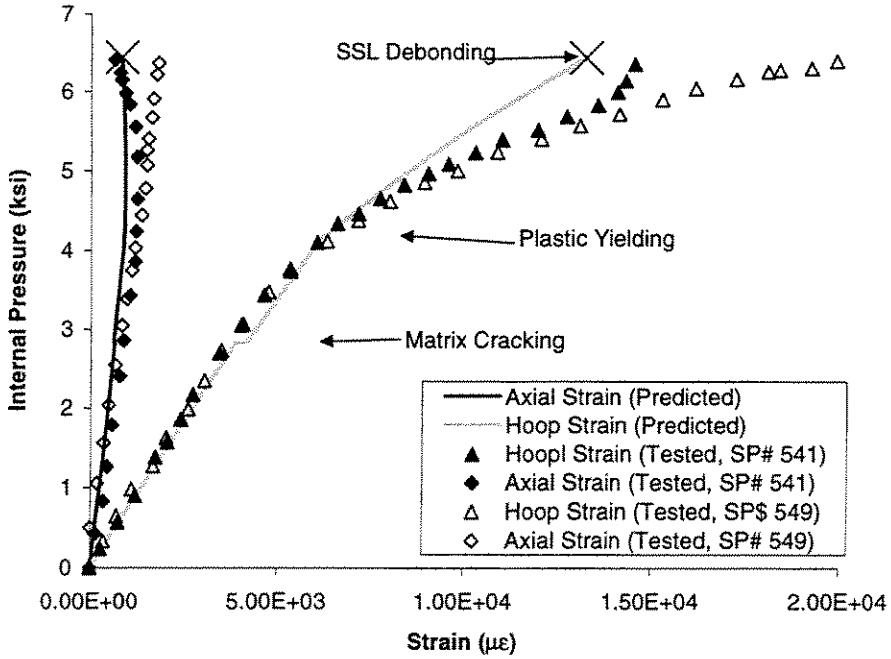

Fig. 6b. Pressure-deformation relationship in 10" 4-strip SSL pipe subjected to combined 2:1 hoop and axial loading at 200°F.

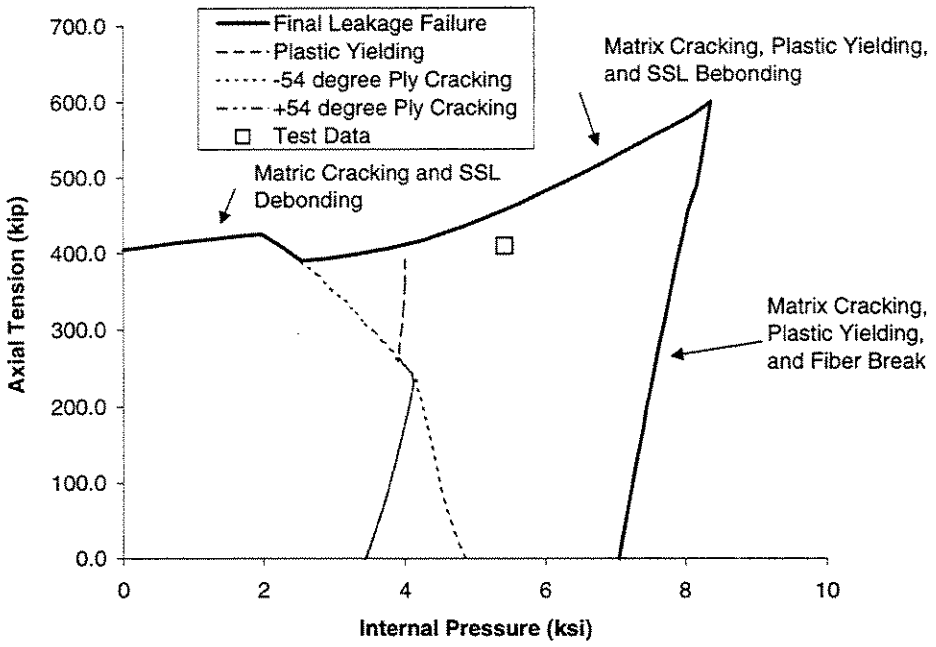

Fig. 7a. Failure modes and leakage failure envelope of 10" 4-strip SSL composite pipe (70°F).

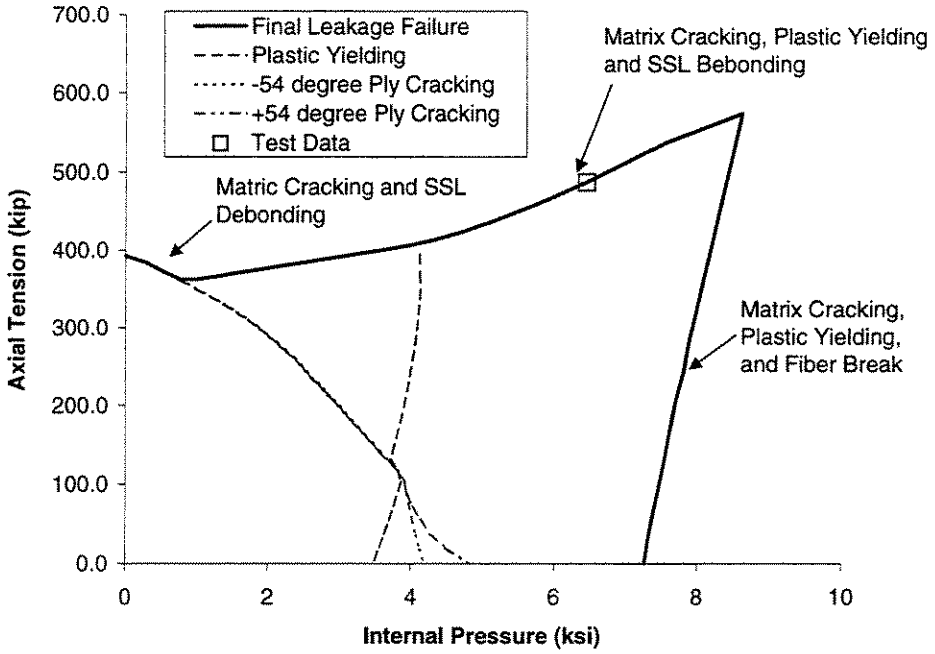

Fig. 7b. Failure modes and leakage failure envelope of 10" 4-strip SSL composite pipe (200°F).

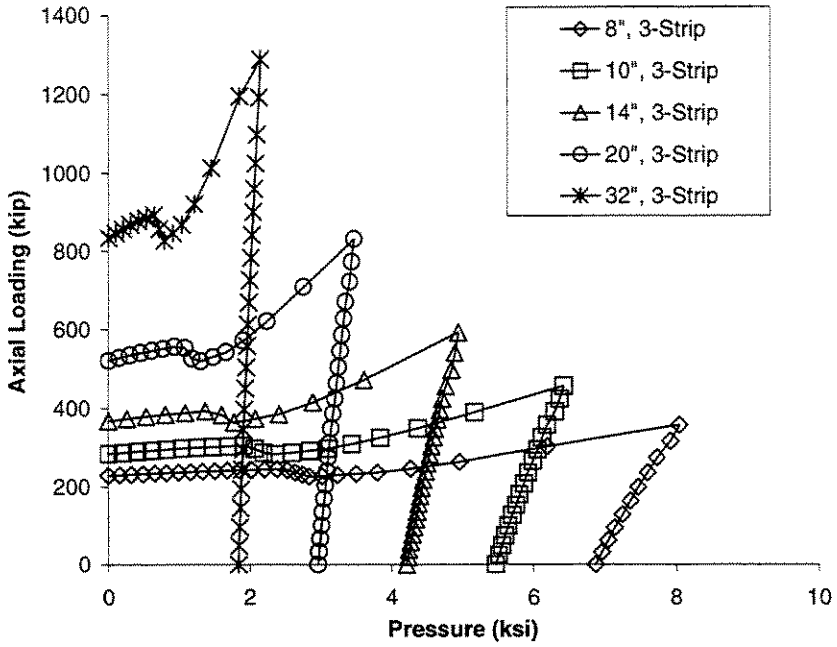

Fig. 8. Leakage failure envelopes of 3-strip SSL composite pipes at room temperature based on applied loads with different diameters.

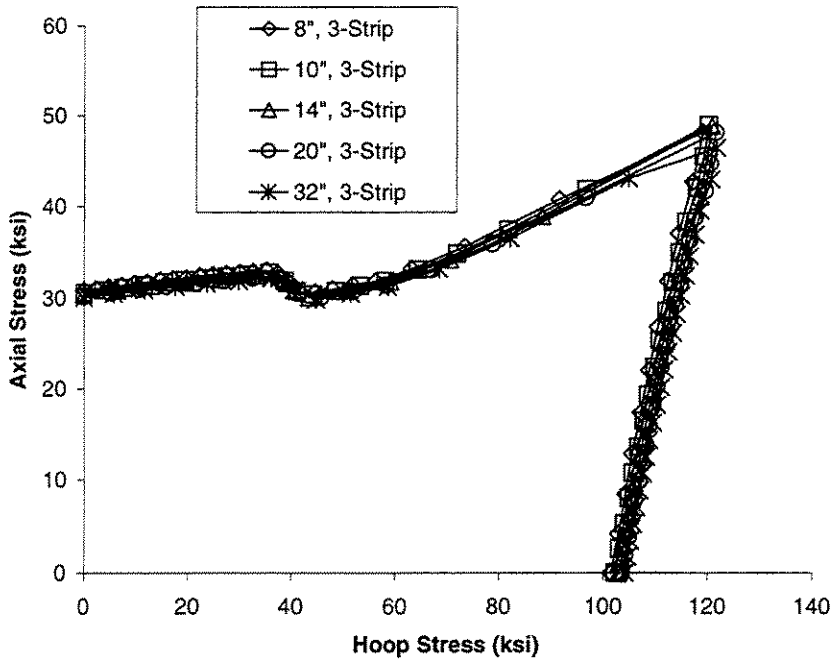

Fig. 9. Leakage failure envelopes of 3-strip SSL composite pipes at room temperature based on average pipe-wall stress.

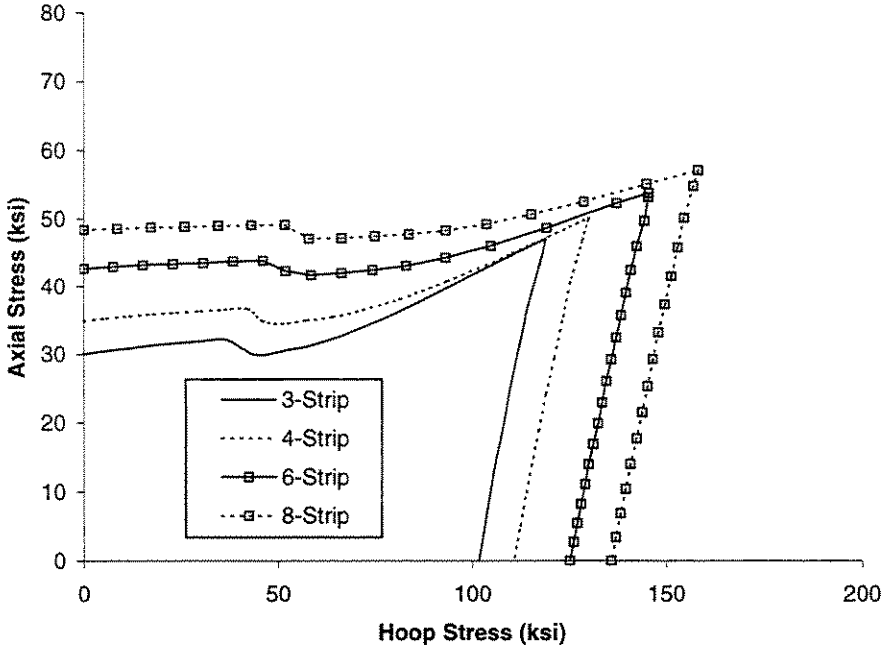

Fig. 10a. Leakage failure envelopes of SSL composite pipes at 70°F.

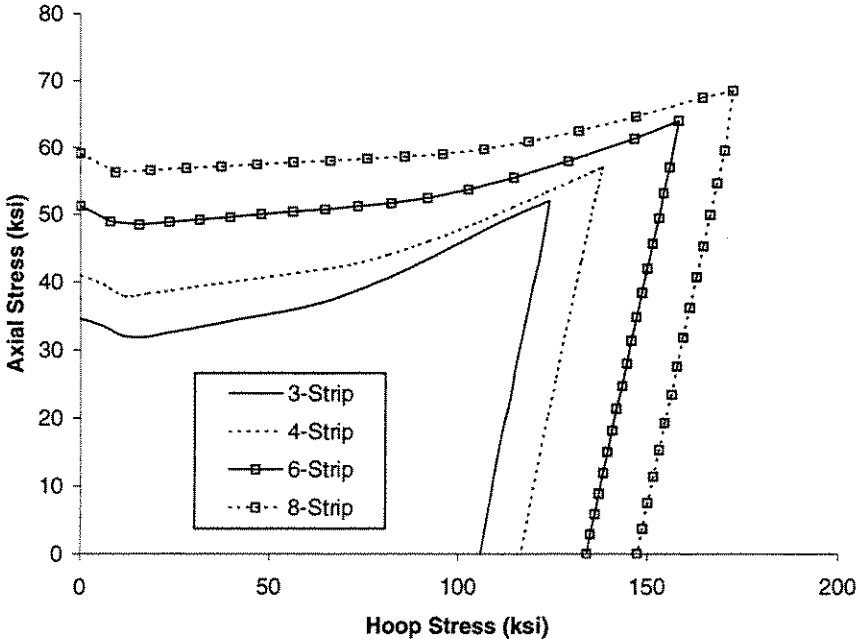

Fig. 10b. Leakage failure envelopes of SSL composite pipes at 200°F.

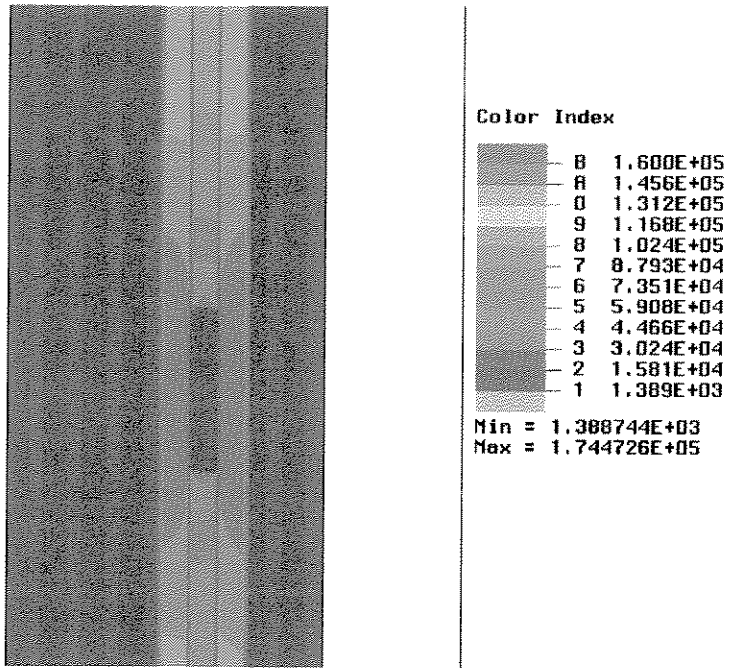

Fig.11a. von Mises stress in SSL pipe subject to 240 kip axial tension. ($\phi = 8$", 3 steel-strip case)

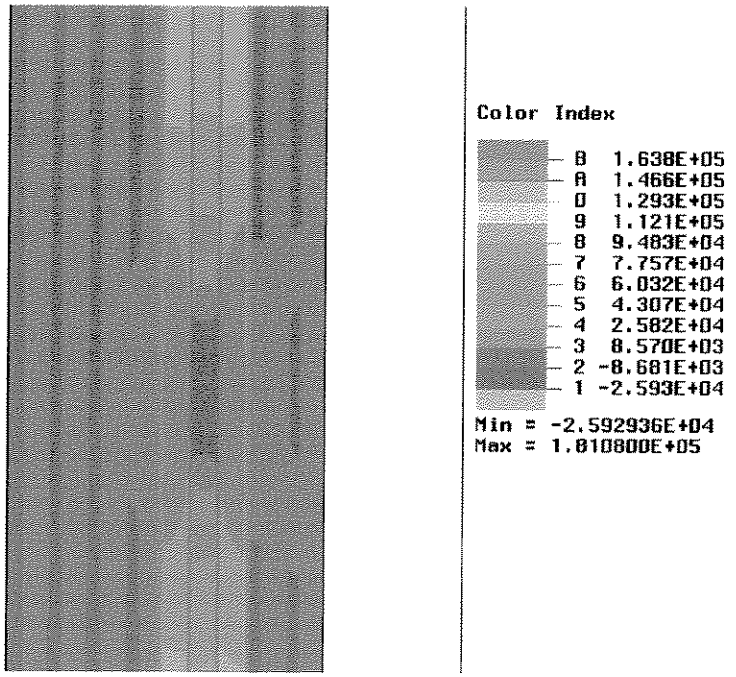

Fig. 11b. $\sigma_{\xi\xi}$ in SSL pipe subject to 240 kip axial tension. ($\phi = 8$", 3 steel-strip case)

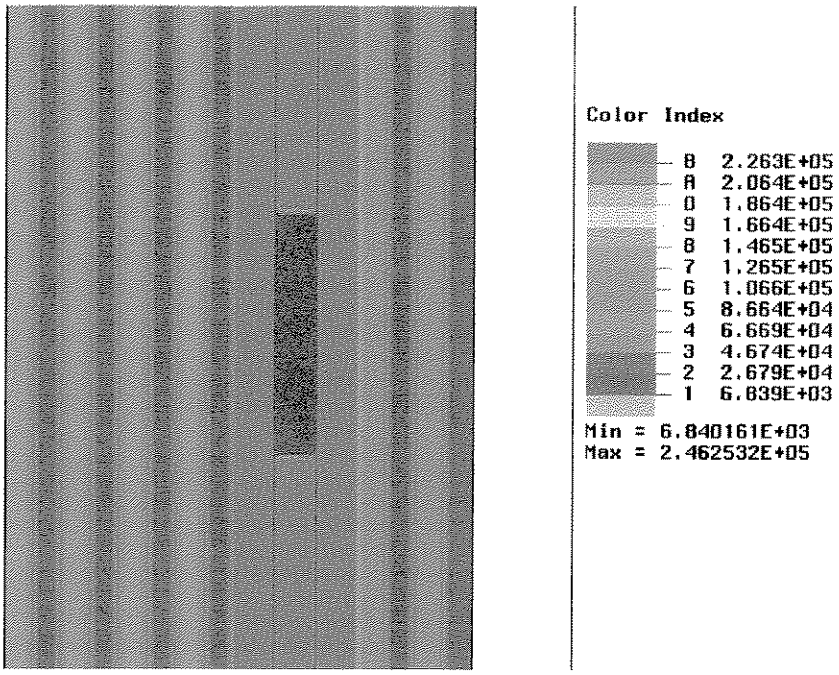

Fig.12a. von Mises stress in SSL pipe subject to 6.9 ksi internal pressure. ($\phi = 8$", 3 steel-strip case)

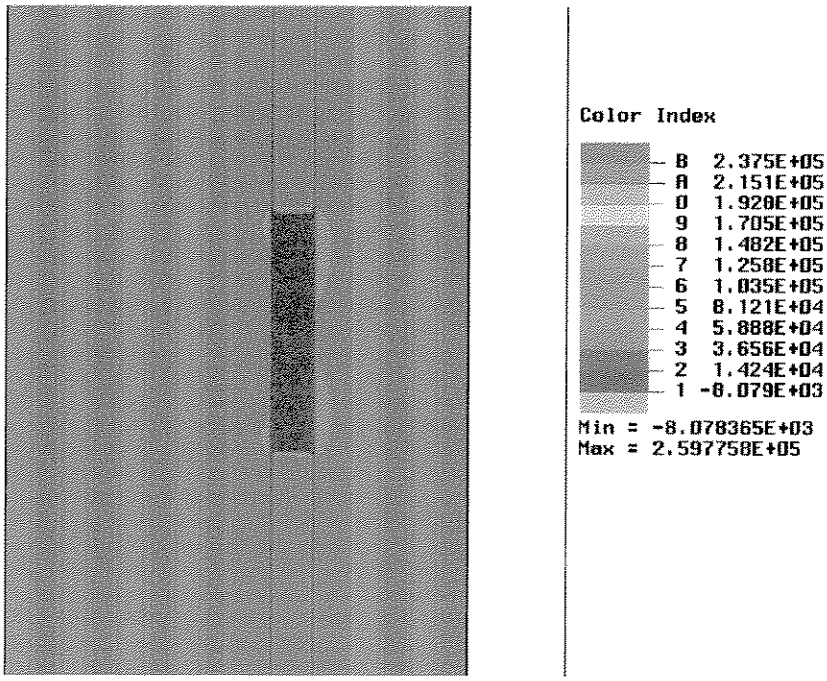

Fig.12b. $\sigma_{\eta\eta}$ in SSL pipe subject to 6.9 ksi internal pressure. ($\phi = 8$", 3 steel-strip case)

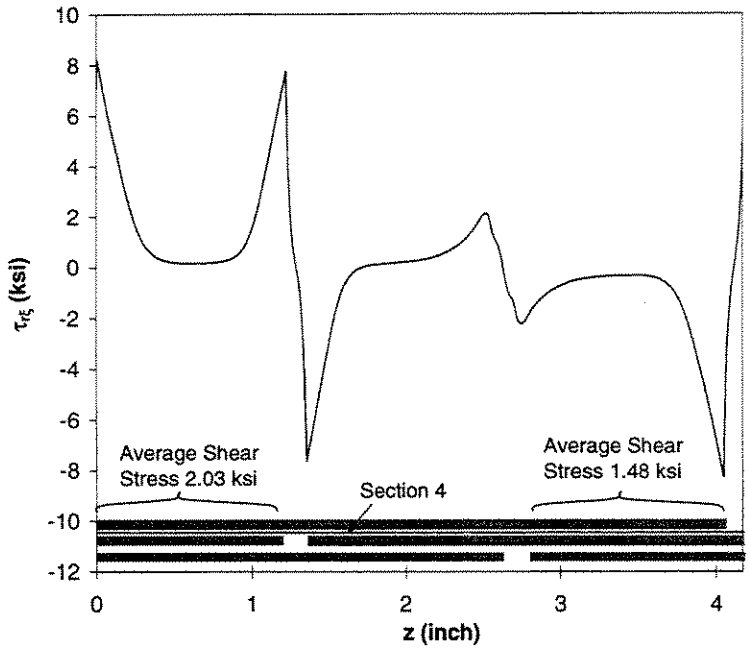

Fig.13a. Shear stress transfer in epoxy adhesive along Section 4 of SSL pipe subject to 240 kip axial tension ($\phi = 8"$, 3 steel-strip case).

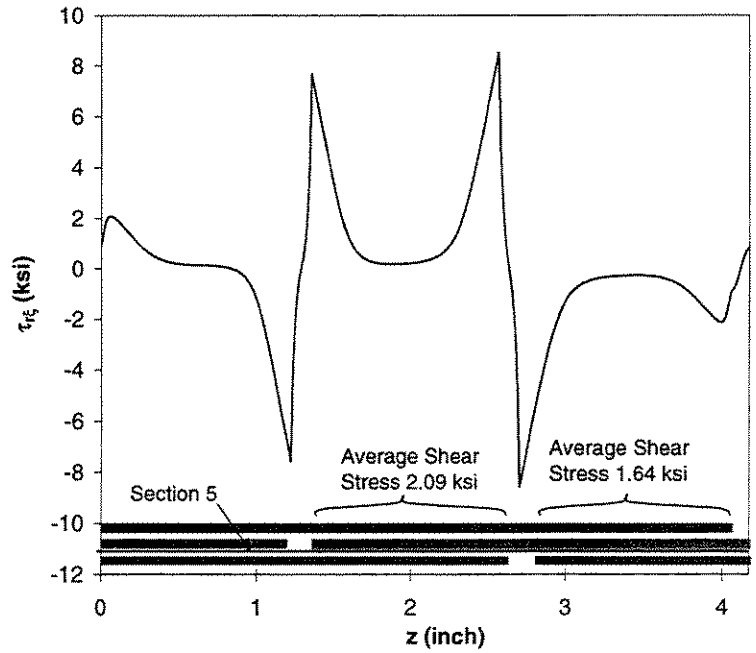

Fig.13b. Shear stress transfer in epoxy adhesive along Section 5 of SSL pipe subject to 240 kip axial tension ($\phi = 8"$, 3 steel-strip case).

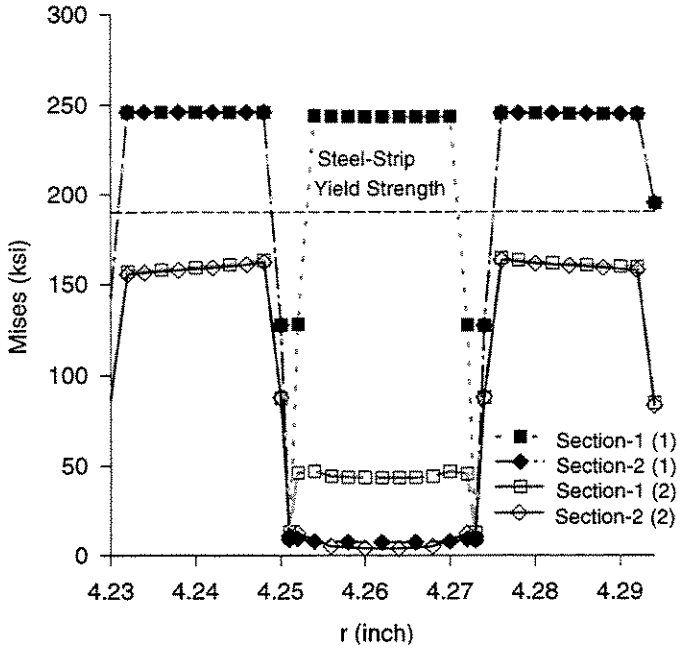

Fig.14a. Von Mises stress along Section 2 in SSL pipe under (1) 6.9 ksi internal pressure, (2) 240 kip axial tension ($\phi = 8$", 3 steel-strip case).

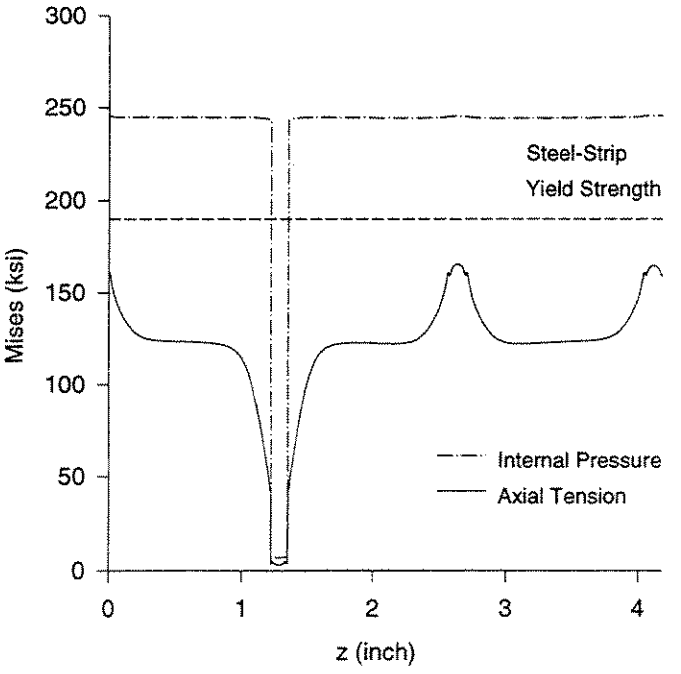

Fig.14b.Von Mises stress along Section 3 in SSL pipe under (1) 6.9 ksi internal pressure, (2) 240 kip axial tension ($\phi = 8$", 3 steel-strip case).